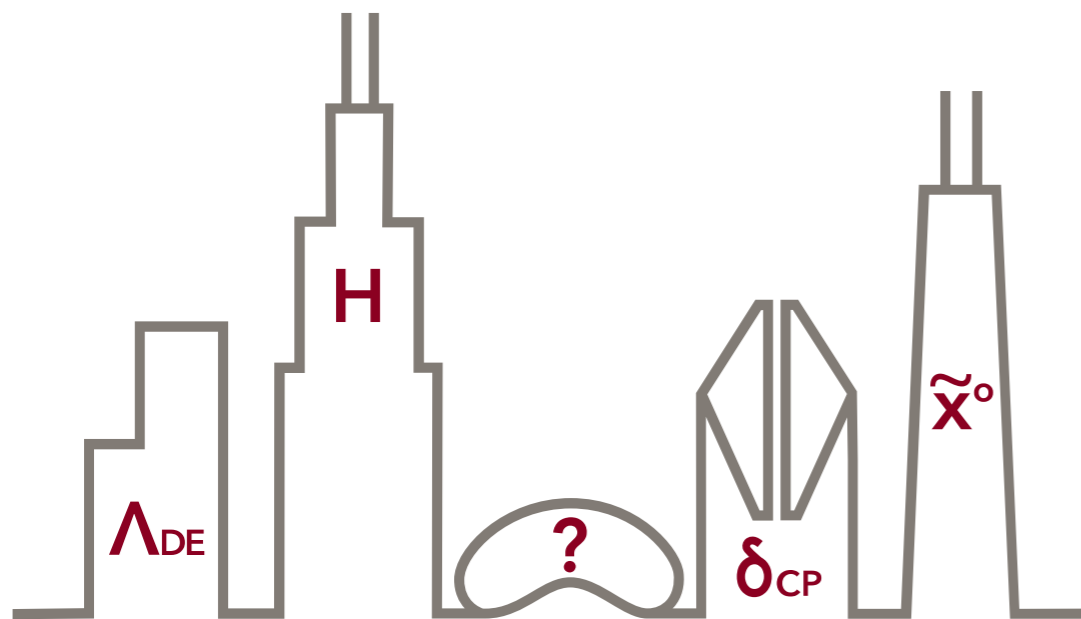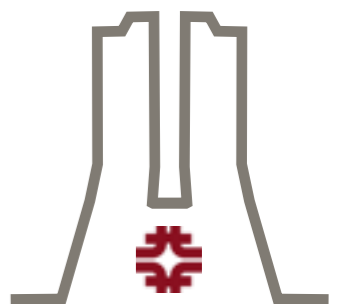# Neutral B(s)-mixing

matrix elements from lattice QCD

for the Standard Model and beyond

Ruth Van De Water standing in for C.M. Bouchard
[Fermilab Lattice and MILC Collaborations]

H

Λ_DE

?

δ_CP

x̃°

⭐ *Material lifted heavily from*
[A.S. Kronfeld talk @ Lattice 2016](#)

The "A (*analysis*)-Team"

Fermilab Lattice & MILC Collaborations

A. Bazavov, C. Bernard, C.M. Bouchard, C.C. Chang, C. DeTar, Daping Du, A.X. El-Khadra, E.D. Freeland, E. Gámiz, Steven Gottlieb, U.M. Heller, A.S. Kronfeld, J. Laiho, P. B. Mackenzie, E. T. Neil, J. Simone, R. Sugar, D. Toussaint, R. S. Van de Water, Ran Zhou

Neutral meson mixing

- In the Standard Model, neutral mesons can oscillate into their antiparticles via 1-loop "box" diagrams:
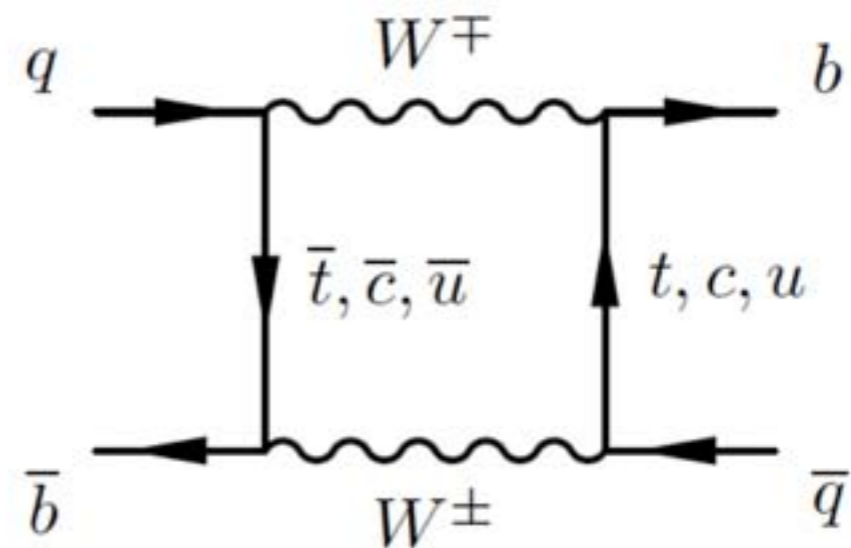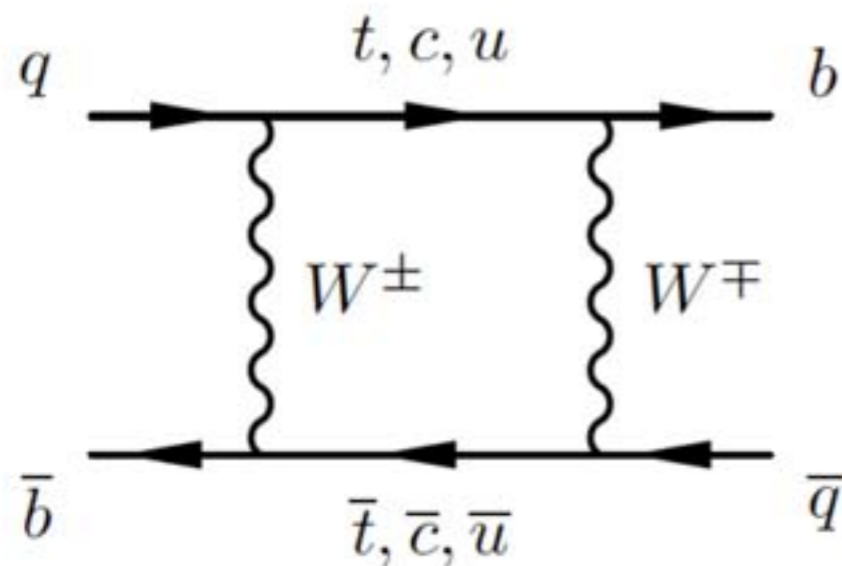
- In extensions of the Standard Model, other particles can appear
  - in the boxes;
  - at tree level (flavor-changing neutral currents).

- Observed experimentally for K^0, D^0, B^0, Bs^0 systems.

ΔB=2 effective Hamiltonian

- GIM mechanism + Cabibbo suppression → top-quark-loop contributions dominant.

- Integrating out (both SM & new) heavy particles above EW scale yields 8 (= 5 + 3) local effective operators:

$$\mathcal{O}_1^q = \bar{b}^\alpha \gamma_\mu L q^\alpha \, \bar{b}^\beta \gamma_\mu L q^\beta \qquad \tilde{\mathcal{O}}_1^q = \bar{b}^\alpha \gamma_\mu R q^\alpha \, \bar{b}^\beta \gamma_\mu R q^\beta$$

$$\mathcal{O}_2^q = \bar{b}^\alpha L q^\alpha \, \bar{b}^\beta L q^\beta \qquad \tilde{\mathcal{O}}_2^q = \bar{b}^\alpha R q^\alpha \, \bar{b}^\beta R q^\beta$$

$$\mathcal{O}_3^q = \bar{b}^\alpha L q^\beta \, \bar{b}^\beta L q^\alpha \qquad \tilde{\mathcal{O}}_3^q = \bar{b}^\alpha R q^\beta \, \bar{b}^\beta R q^\alpha$$

$$\mathcal{O}_4^q = \bar{b}^\alpha L q^\alpha \, \bar{b}^\beta R q^\beta$$

$$\mathcal{O}_5^q = \bar{b}^\alpha L q^\alpha \, \bar{b}^\beta R q^\alpha$$

- By parity of QCD: $\langle \bar{B}_q | \tilde{\mathcal{O}}_i^q | B_q \rangle = \langle \bar{B}_q | \mathcal{O}_i^q | B_q \rangle$, leaving 5.

- Lattice calculations of matrix elements $\langle O^q_i \rangle$ (q=d,s; i=1–5) sufficient to characterize hadronic contributions to $B_{(s)}$-mixing in SM and beyond.
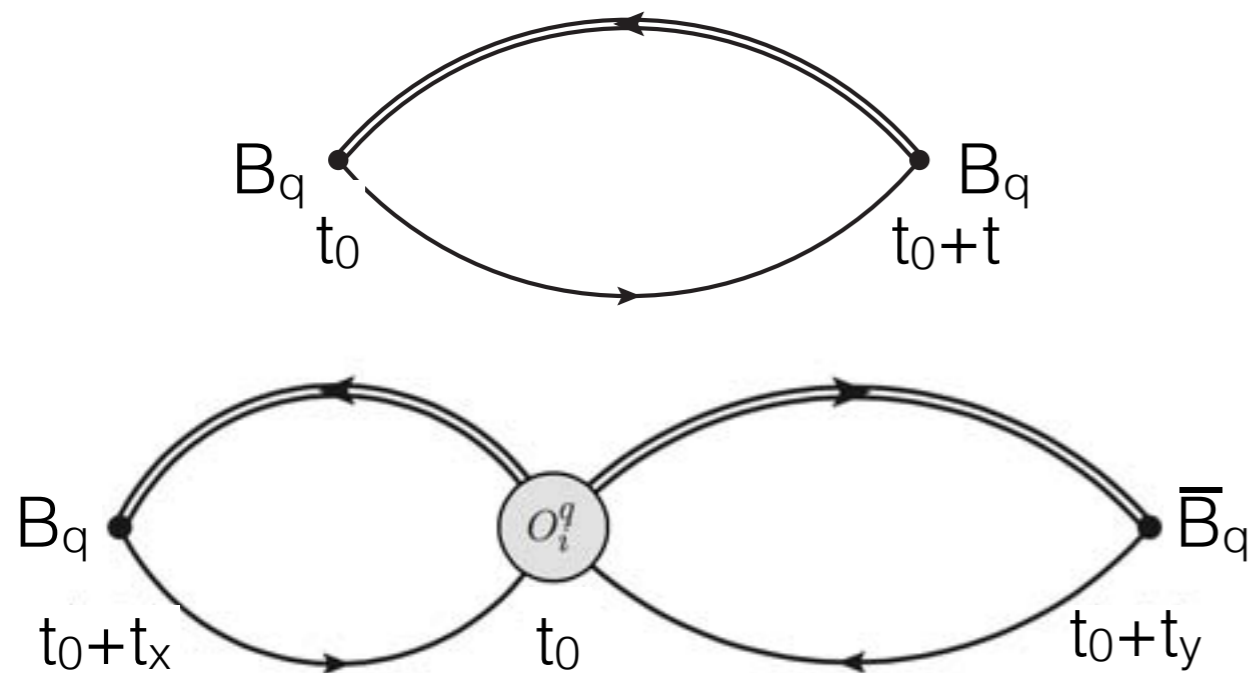
Lattice simulations

MILC staggered gauge-field ensembles with 3 dynamical quarks (u,d,s).

- 600 - 2200 gauge-field configurations per ensemble
- 4 lattice spacings
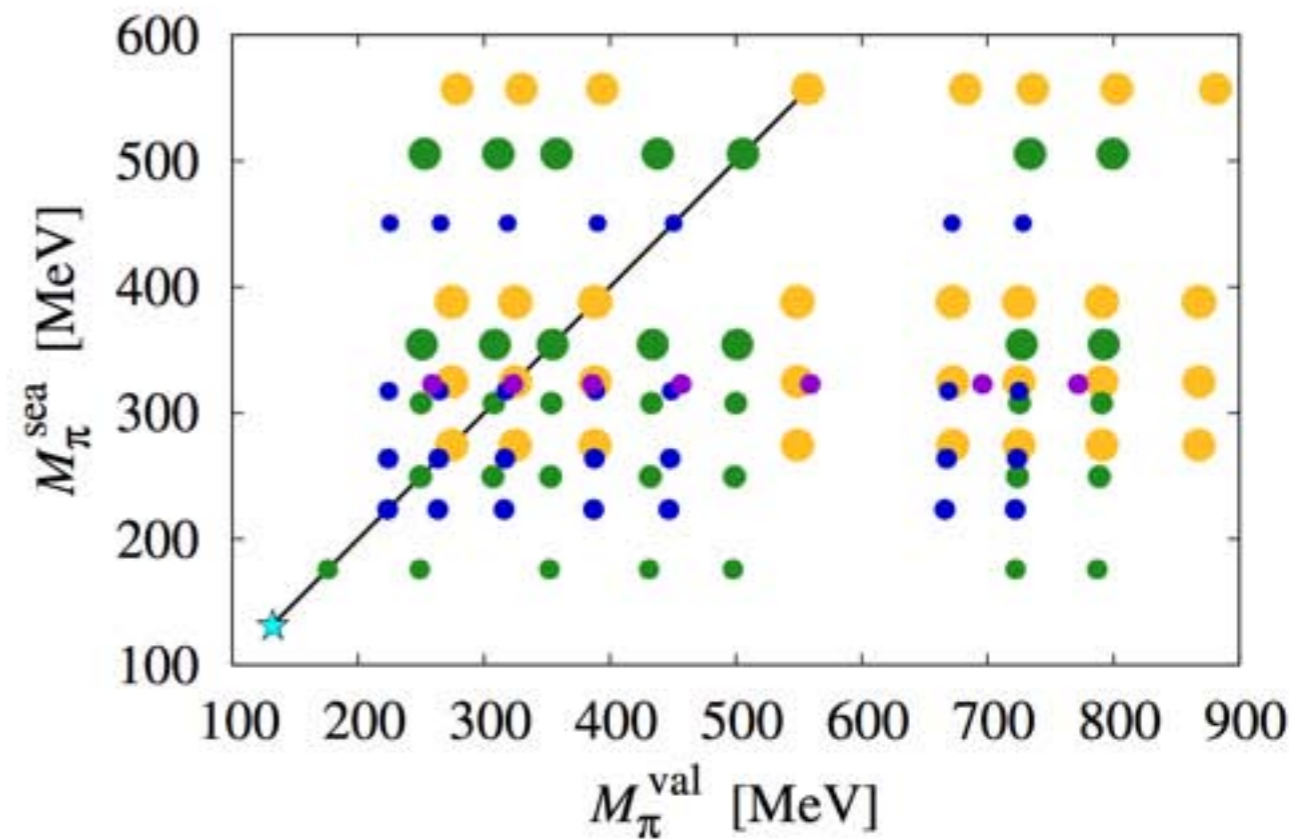- lightest pion mass M_π = 177 MeV close to physical value

5
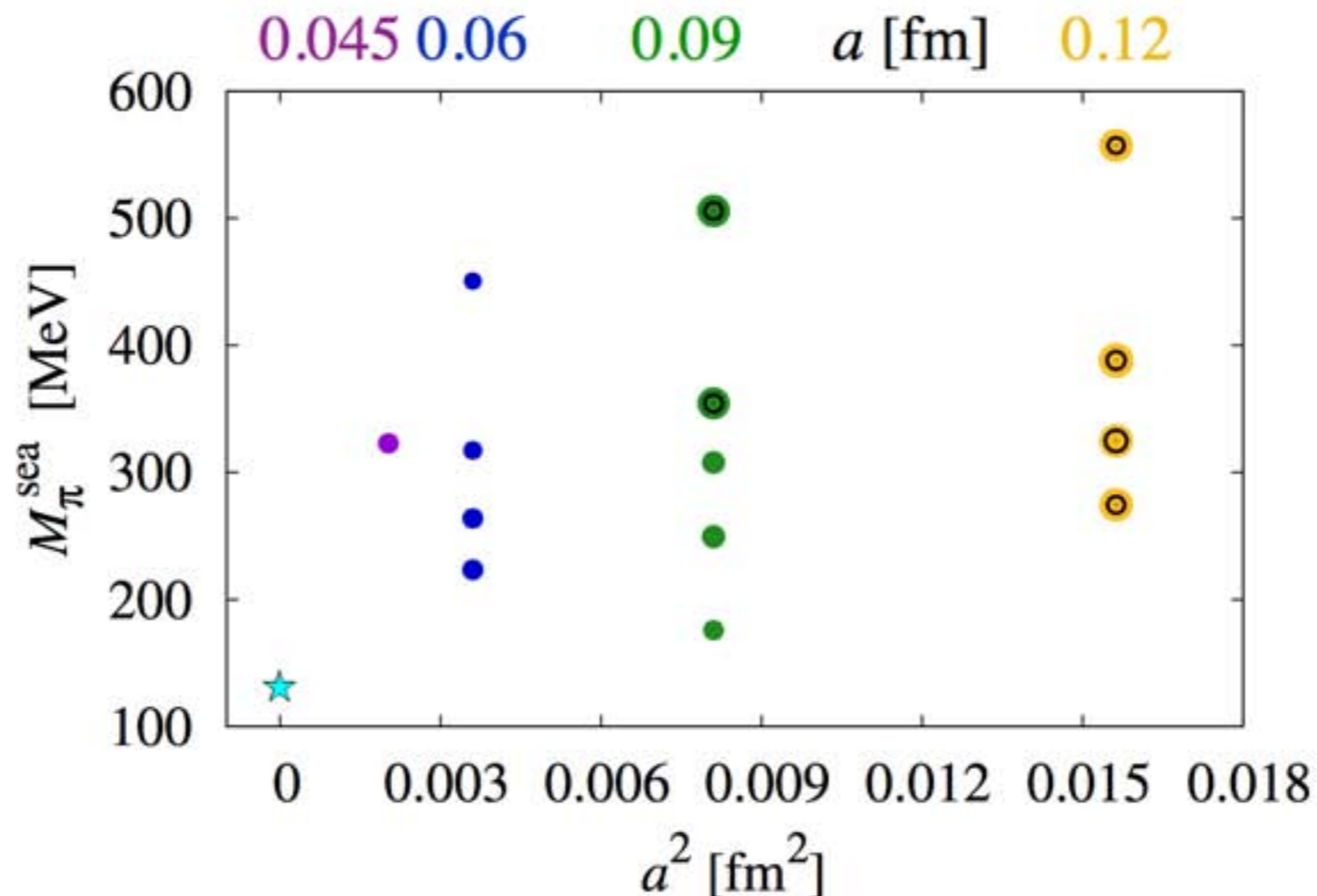
Lattice correlation functions

2- and 3-point correlators

Valence light-quark masses

Relativistic b quarks with Fermilab action.

Light-quark masses (m_q) in B_q mesons independent of sea-quark masses in gauge-field configurations.

- multiple m_q on each ensemble improve extrapolation to physical M_π.

Renormalize and match lattice operators O_i^q to continuum $\overline{MS}$-NDR scheme using mostly nonperturbative renormalization.

Chiral-continuum extrapolation

nonanalytic "chiral logarithm" terms from NLO HMrSχPT

heavy-quark discretization effects (derived in HQET)

fine tune simulation *b*-quark mass

$$F_i = F_i^{\text{logs}} + F_i^{\text{analytic}} + F_i^{\text{HQ disc}} + F_i^{\alpha_s a^2 \text{ gen}} + F_i^{\kappa} + F_i^{\text{renorm}}$$
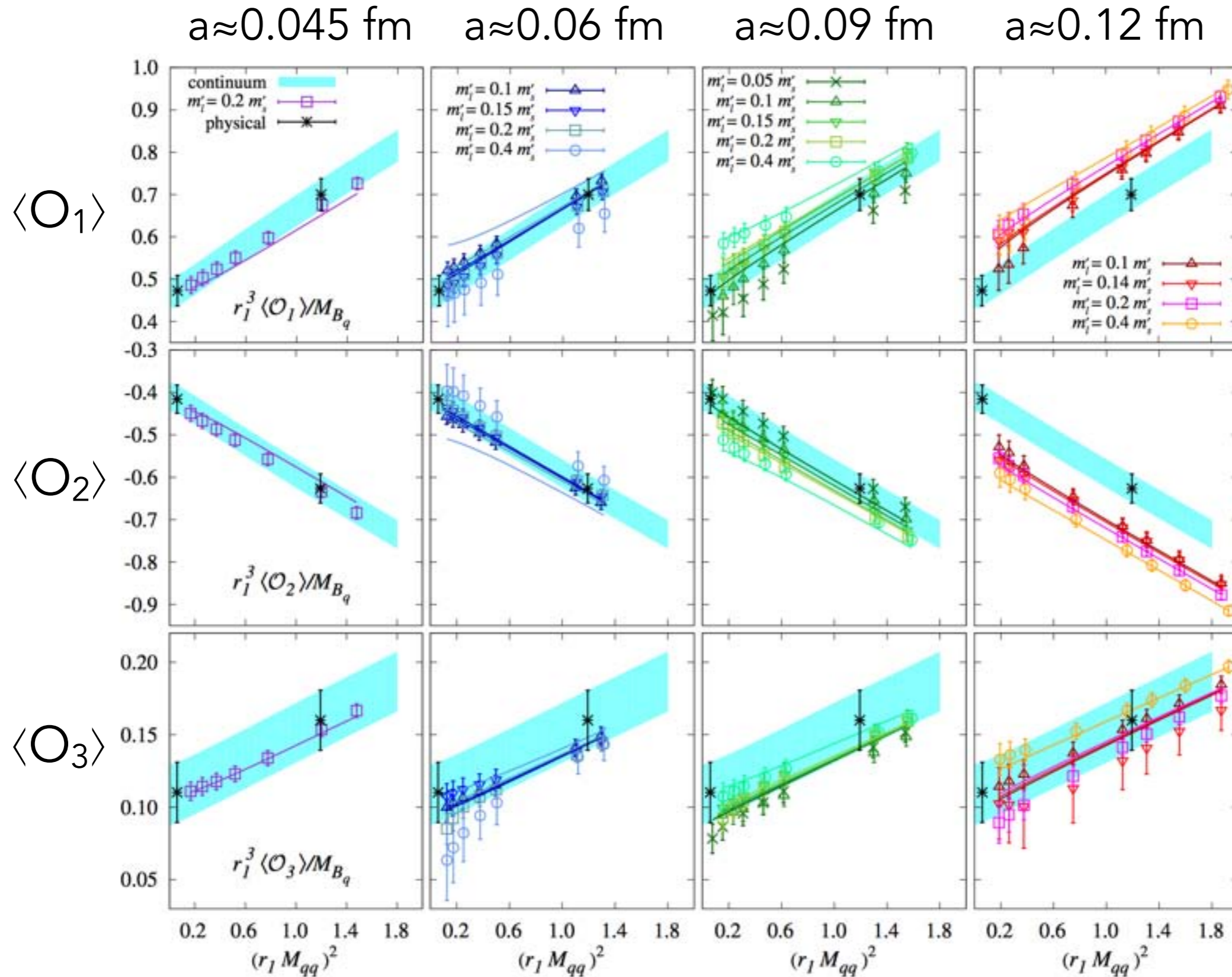
analytic terms of N^{n}LO in χPT (*n=2 in central fit*)

gluon & light-quark discretization effects (via Symanzik EFT)

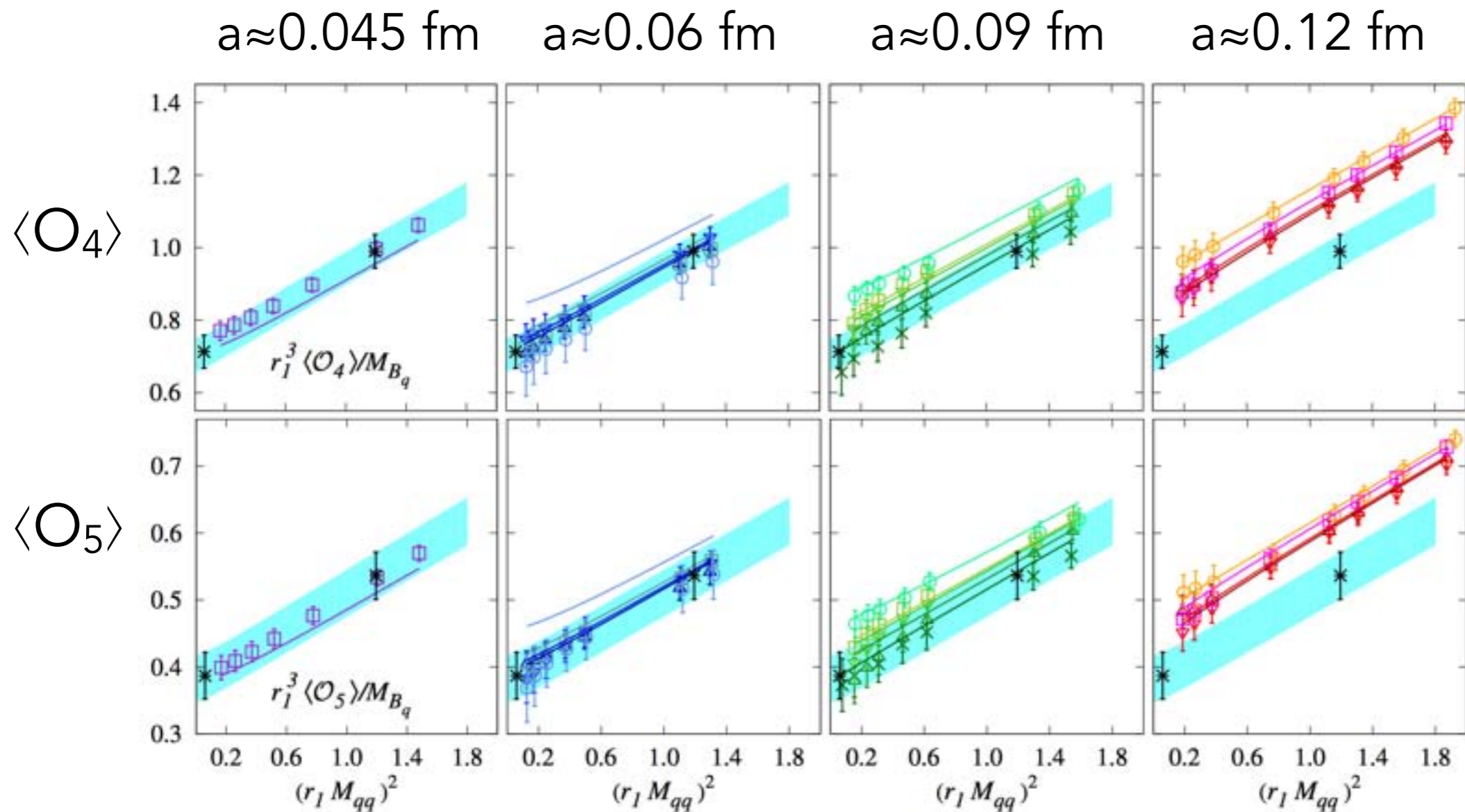fit O(α_s^2) terms to data to constrain size

- **Simultaneous, correlated fit of all data**: 5 operators, valence- & sea-quark masses, and lattice spacings.

Fit results for $\langle O_1 \rangle - \langle O_3 \rangle$

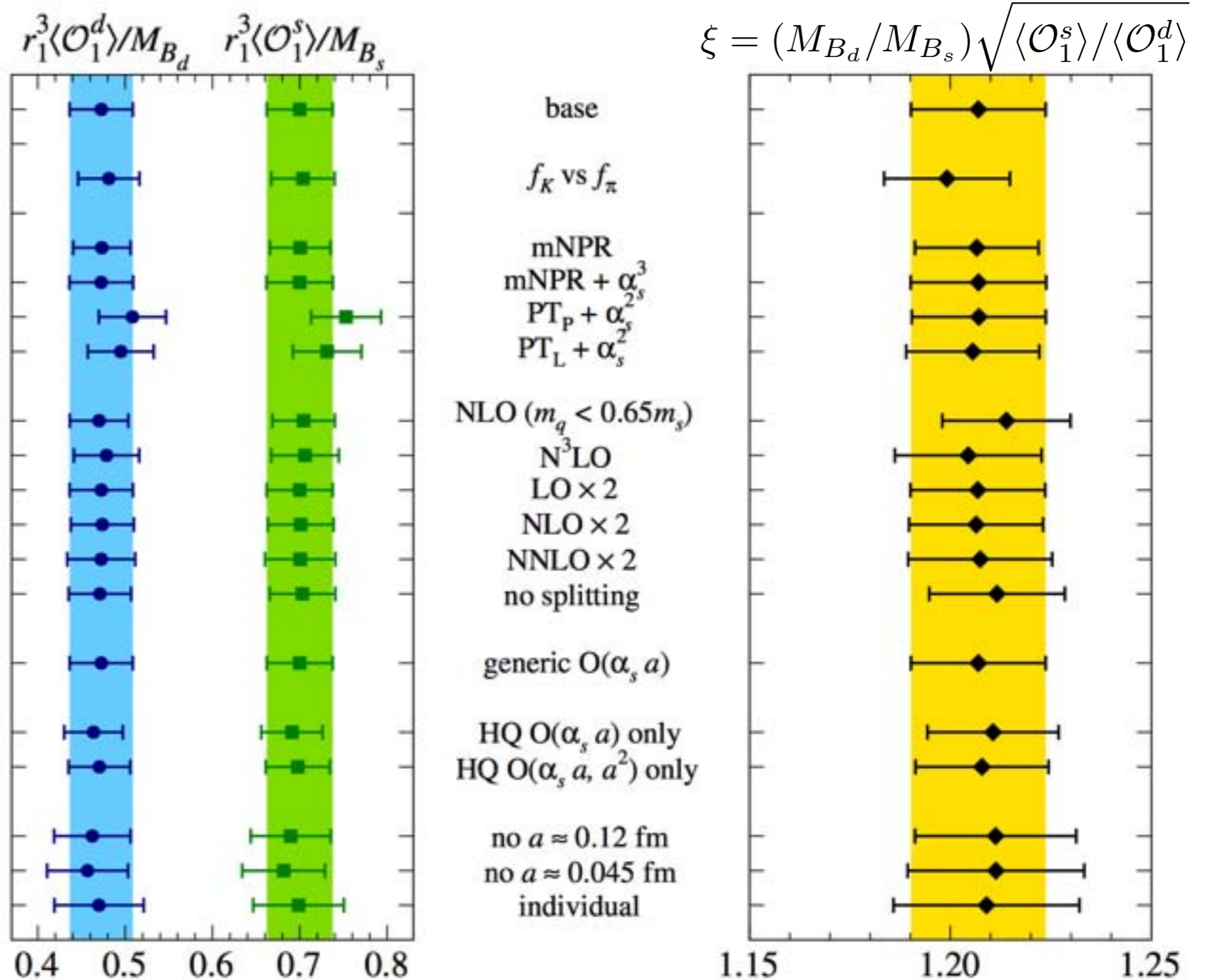# Fit results for $\langle O_4 \rangle$ & $\langle O_5 \rangle$

$$\chi^2_{\text{aug}}/\text{dof} = 134.9/510$$

Stability under fit variations

- f_K instead of f_π

- vary operator renormalization

- vary data, χPT terms, prior widths

- vary discretization terms included

- "dumb" fits

Fit error encompasses uncertainties from perturbative matching, truncating the chiral expansion, & discretization errors.

Results for Standard-Model operator $\langle O_1 \rangle$

$$f^2_{B_d}\hat{B}^{(1)}_{B_d} = 0.0518(43)_{\text{total}}(10)_{\text{charm sea}} \text{ GeV}^2$$

$$f^2_{B_s}\hat{B}^{(1)}_{B_s} = 0.0754(46)_{\text{total}}(15)_{\text{charm sea}} \text{ GeV}^2$$

$$\xi = 1.206(18)_{\text{total}}(6)_{\text{charm sea}}$$

- SU(3)-breaking ratio ξ ~3× more precise than previous calculations.
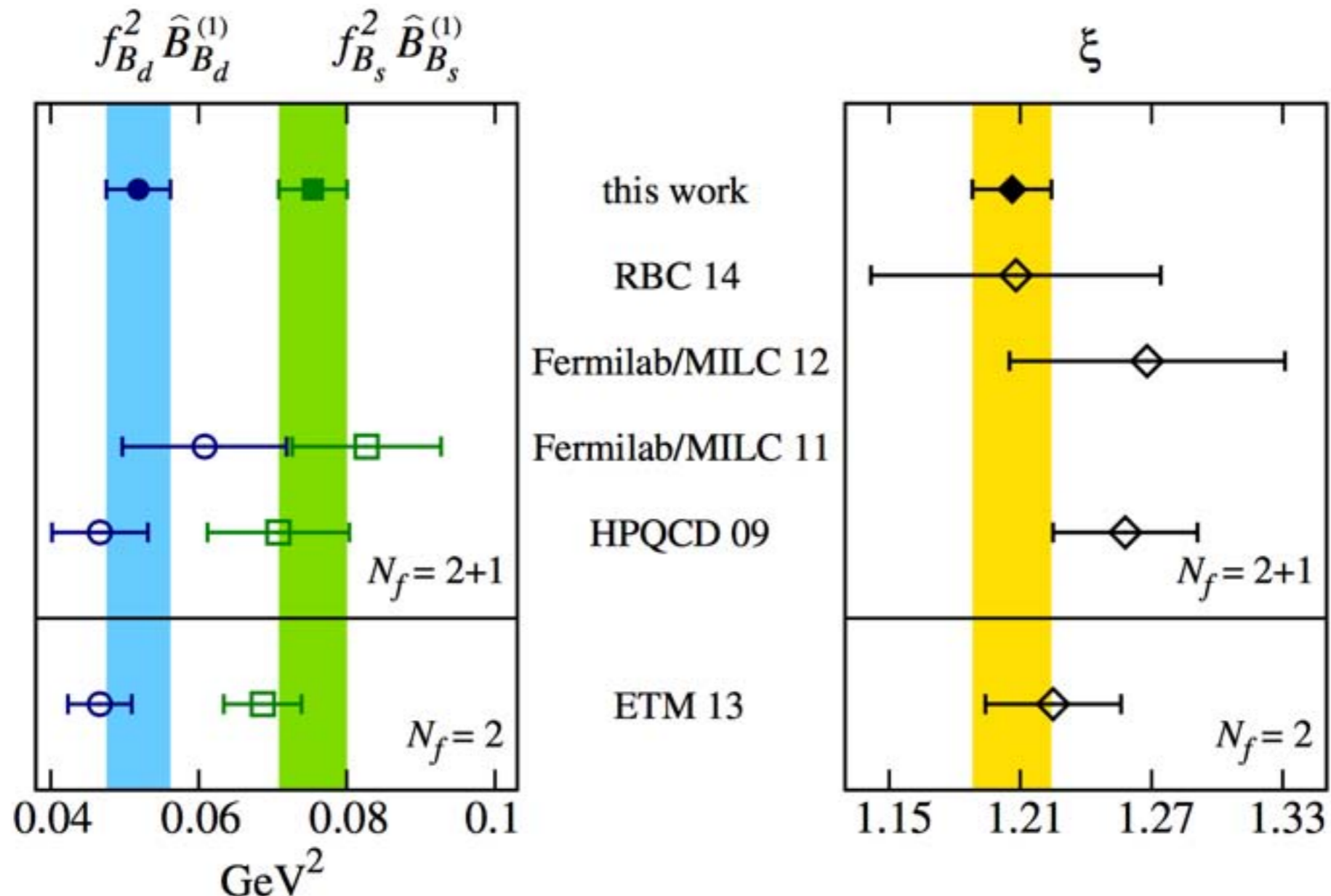
Full set of ΔB=2 matrix elements

- ETM results from $N_f = 2$ simulations [JHEP 1403 (2014) 016]; uncertainties do not include error from omission of strange sea quarks.

Standard-Model B$_{(s)}^0$-meson oscillation frequencies

$$\Delta M_d^{\mathrm{SM}} = 0.630(53)_{\mathrm{LQCD}}(42)_{\mathrm{CKM}}(5)_{\mathrm{other}}(13)_{\mathrm{charm\ sea}}\ \mathrm{ps}^{-1}$$
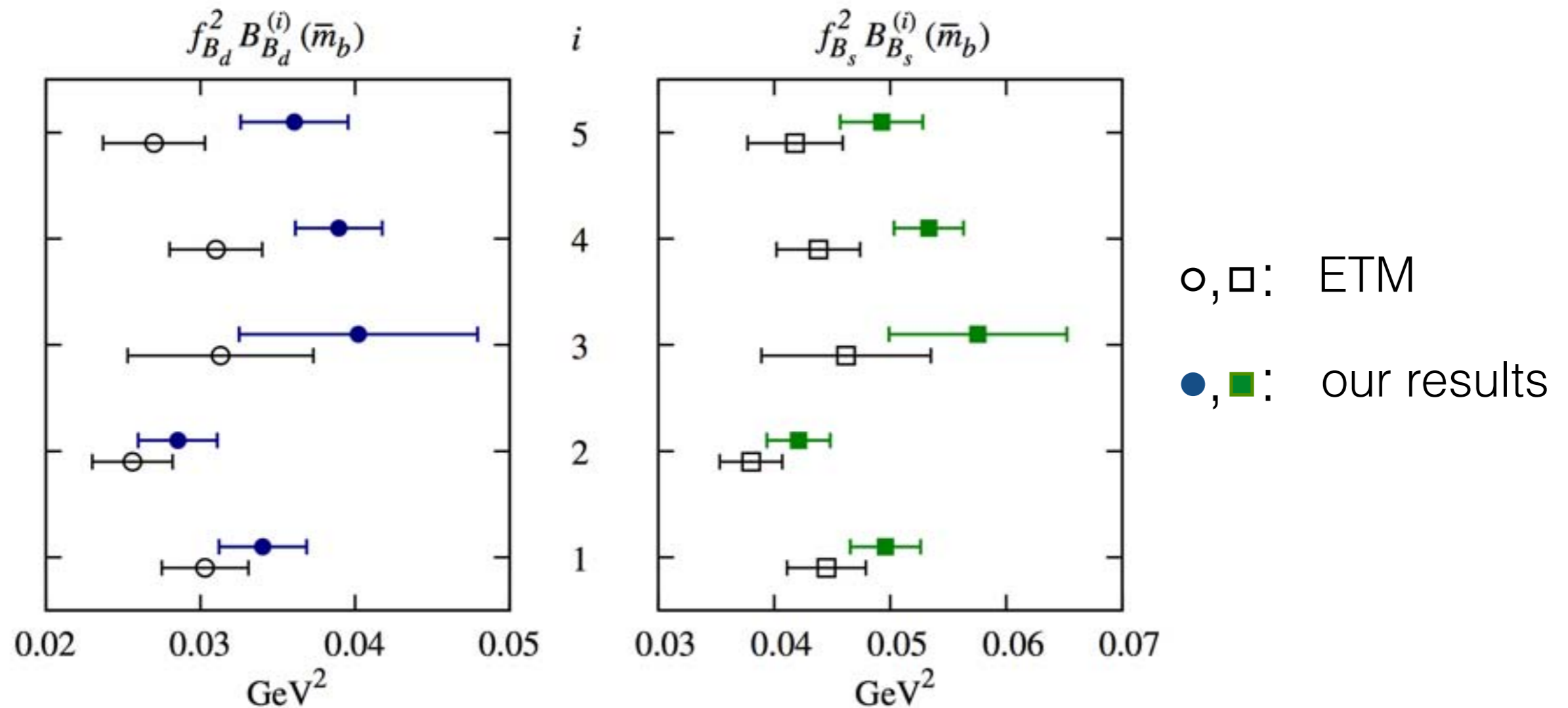
$$\Delta M_s^{\mathrm{SM}} = 19.6(1.2)_{\mathrm{LQCD}}(1.0)_{\mathrm{CKM}}(0.2)_{\mathrm{other}}(0.4)_{\mathrm{charm\ sea}}\ \mathrm{ps}^{-1}$$

$$\left(\frac{\Delta M_d}{\Delta M_s}\right)^{\mathrm{SM}} = 0.0321(10)_{\mathrm{LQCD}}(15)_{\mathrm{CKM}}(3)_{\mathrm{other}}$$

using determinations of CKM factors $|V_{td}\,V_{tb}^*|$ and $|V_{ts}\,V_{tb}^*|$ from tree-level processes. [CKMfitter Group (Descotes-Genon, *private comm.*)]

- Differ from measurements by 2.1σ, 1.3σ, and 2.9σ, respectively.

$$\Delta M_d^{\mathrm{expt}} = 0.5055(20)\ \mathrm{ps}^{-1}$$

$$\Delta M_s^{\mathrm{expt}} = 17.757(21)\ \mathrm{ps}^{-1}$$

- Alternatively, use $\Delta M_q^{\mathrm{exp}}$ and determine CKM factors (*assuming no new physics in B$_{(s)}^0$-meson oscillations...*)

Implications for CKM matrix elements
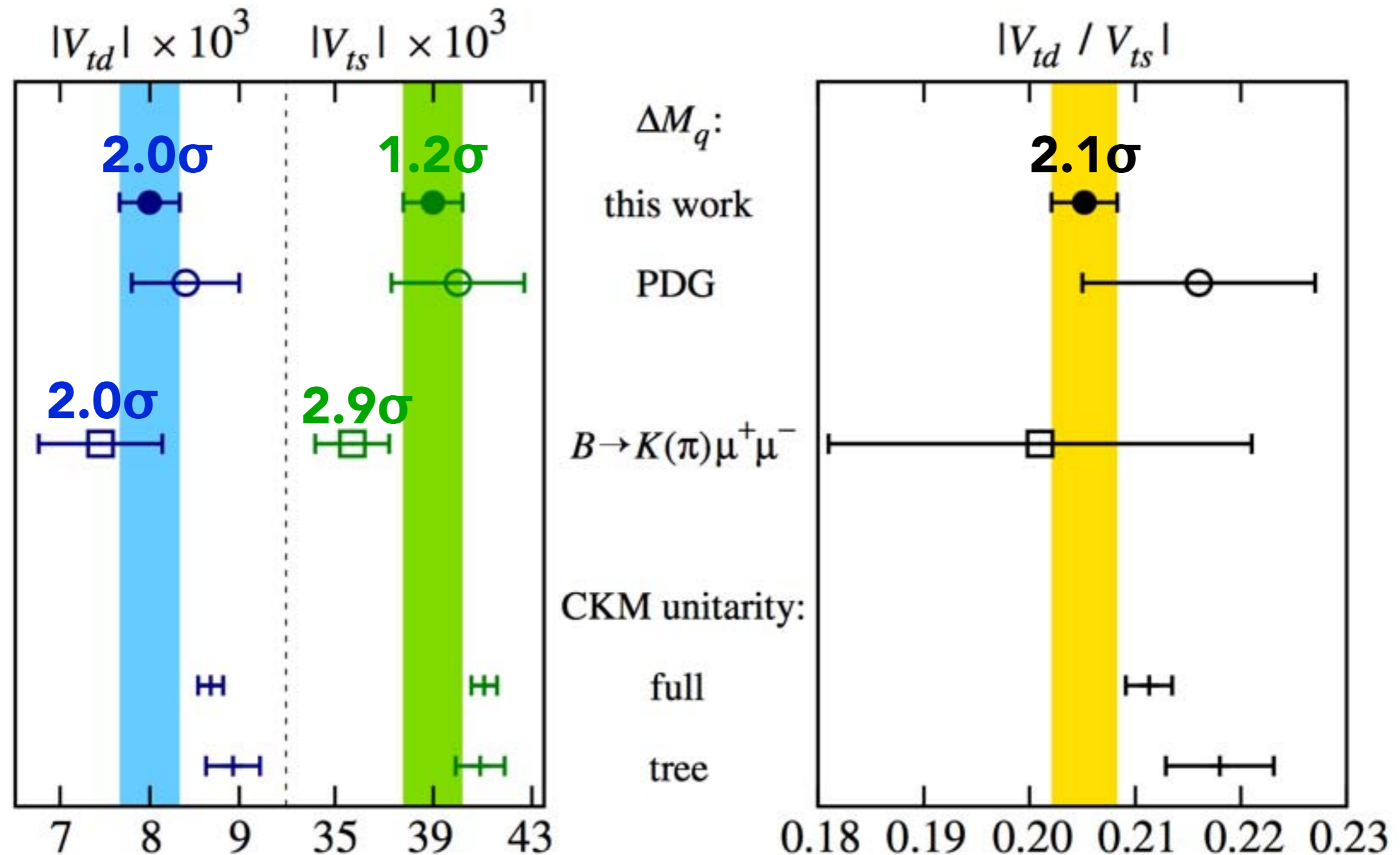
Determinations from flavor-changing-neutral-current processes differ by ~2σ from values implied by tree-level processes + CKM unitarity.

Impact on CKM unitarity-triangle fit

Using Fermilab/MILC results for $B_{(s)}$ mixing, $|V_{cb}|$ from $B{\to}Dl\nu$ [arXiv:1503.07237], and $|V_{ub}|$ from $B{\to}\pi l\nu$ [arXiv:1503.07839].

Plot by
E. Lunghi

Rare $B_{(s)}^0 \rightarrow \mu^+\mu^-$ leptonic decay rates

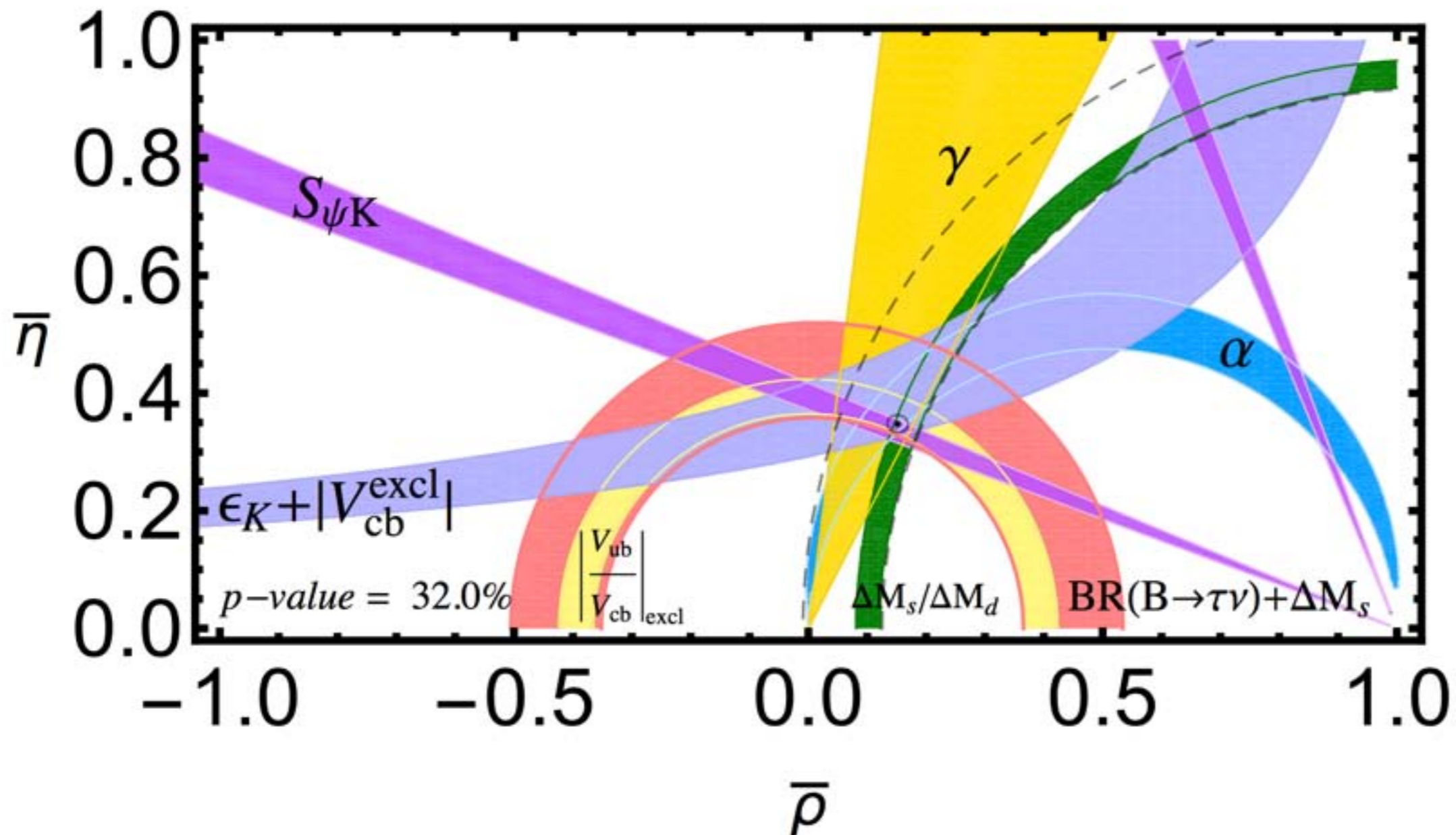Standard Model ratios of B_q^0-meson leptonic decay rates to oscillation frequencies $BR(B_q^0 \rightarrow \mu^+\mu^-)/\Delta M_q$ independent of CKM factors $|V_{tq}V_{tb}^*|$ [Buras PLB566, 115 (2003), Bobeth *et al.* PRL112, 101801 (2014)]

- combine with ΔM_q^{exp} to obtain $BR(B_q^0 \rightarrow \mu^+\mu^-)$

$$\bar{\mathcal{B}}(B_d \rightarrow \mu^+\mu^-)^{\mathrm{SM}} \times 10^{11} = 9.06(87) \qquad \bar{\mathcal{B}}(B_s \rightarrow \mu^+\mu^-)^{\mathrm{SM}} \times 10^9 = 3.22(23)$$
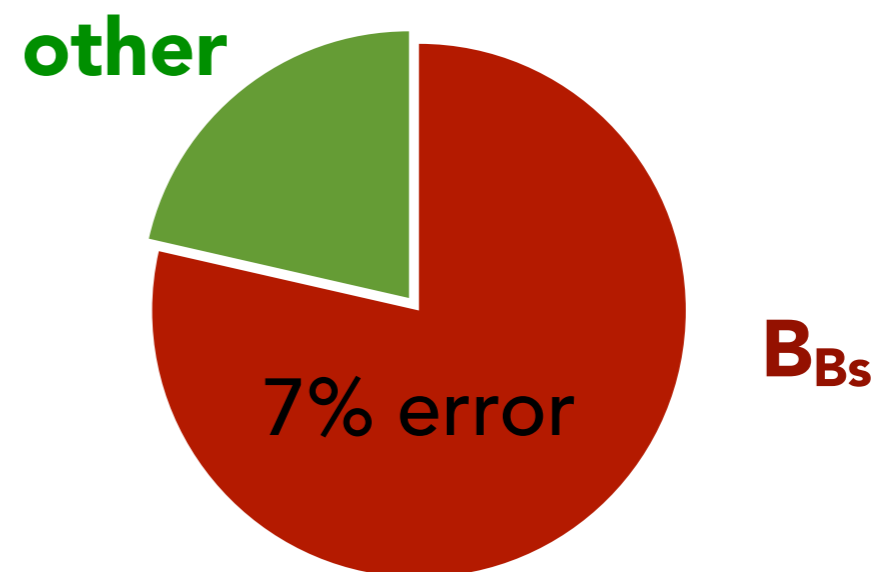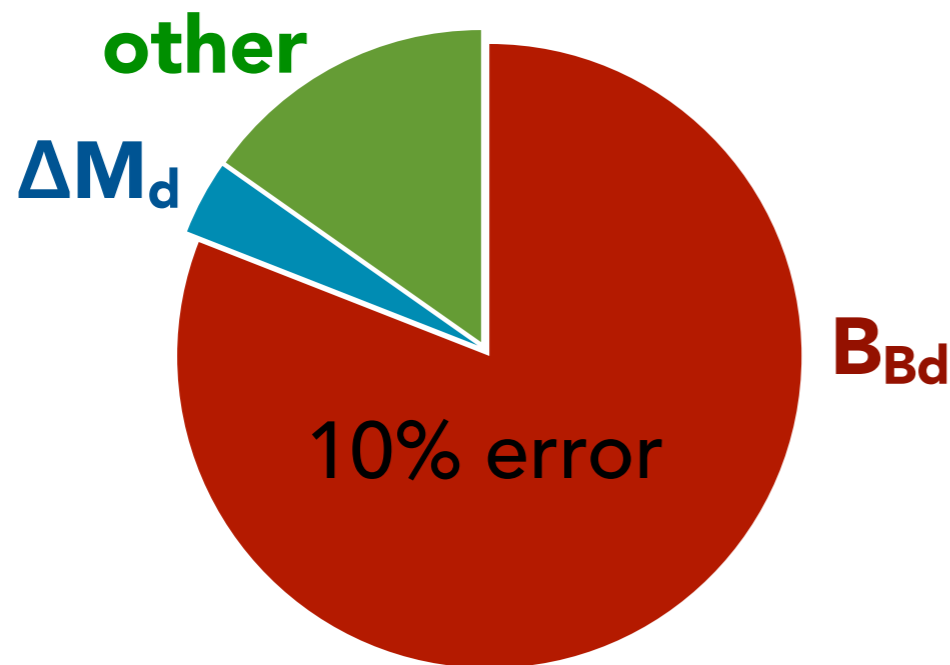
Agrees with measurement $BR(B_s^0 \rightarrow \mu^+\mu^-)^{exp} \times 10^9 = 2.8(+7,-6)$ [LHCb & CMS, Nature 522, 68 (2015), arXiv:1411.4413].

Summary & outlook

First 3-flavor results for full set of ΔB=2 local $B_{(s)}$-mixing matrix elements.

- and first calculation of SM matrix elements $\langle O_1^{d,s} \rangle$ with all systematic errors controlled.
- error on SU(3) breaking ratio ξ reduced by factor of 3.

New matrix elements reveal several ~2σ tensions with Standard Model.

- similar-sized deviations observed in b→d,s FCNC semileptonic decays B→ π (K)μ⁺μ⁻ decays.
- *emerging tension between tree- and loop-level weak processes?*

Working to bring QCD errors to level of experimental measurements.

- analysis of 4-flavor MILC HISQ ensembles with physical u/d-quark masses, finer lattice spacings, and charm sea quarks will eliminate chiral extrapolation and reduce b-quark discretization errors.
- 4-flavor calculation by HPQCD using NRQCD b quarks also underway [arXiv:1411.6989]

details...

TABLE XIII. B_q-mixing matrix elements $f_{B_q}^2 B_{B_q}^{(i)}$ in the $\overline{\mathrm{MS}}$-NDR scheme evaluated at the scale $\mu = \overline{m}_b$, with total statistical plus systematic uncertainties. The first error is the "Total" error listed in Table XI and the second is the "charm sea" error listed in the last column of that table. For operators $\mathcal{O}_2^q$ and $\mathcal{O}_3^q$, results for both the BMU [124] and BBGLN [67, 123] evanescent-operator conventions are shown. Entries are in GeV^2.

	$B_d\text{–}\bar{B}_d$		$B_s\text{–}\bar{B}_s$	
	BMU	BBGLN	BMU	BBGLN
$f_{B_q}^2 B_{B_q}^{(1)}(\overline{m}_b)$	0.0342(29)(7)		0.0498(30)(10)	
$f_{B_q}^2 B_{B_q}^{(2)}(\overline{m}_b)$	0.0285(26)(6)	0.0303(27)(6)	0.0421(27)(8)	0.0449(29)(9)
$f_{B_q}^2 B_{B_q}^{(3)}(\overline{m}_b)$	0.0402(77)(8)	0.0399(77)(8)	0.0576(77)(12)	0.0571(77)(11)
$f_{B_q}^2 B_{B_q}^{(4)}(\overline{m}_b)$	0.0390(28)(8)		0.0534(30)(11)	
$f_{B_q}^2 B_{B_q}^{(5)}(\overline{m}_b)$	0.0361(35)(7)		0.0493(36)(10)	

Bag-parameters results

TABLE XV. Upper panel: $B_{B_q}^{(i)}(\mu)$ in the $\overline{\text{MS}}$-NDR scheme evaluated at the scale $\mu = \overline{m}_b$ with evanescent operator scheme specified by BMU or BBGLN. Errors shown are from the matrix elements in Table XIII and from the decay constants, respectively. Lower panel: ratios of bag parameters $B_{B_q}^{(i)}(\overline{m}_b)/B_{B_q}^{(1)}(\overline{m}_b)$ (i=2–5). Errors are from the matrix elements in Table XIII, and...

	B_d–$\bar{B}_d$		B_s–$\bar{B}_s$	
	BMU	BBGLN	BMU	BBGLN
$B_{B_q}^{(1)}(\overline{m}_b)$	0.913(76)(40)		0.952(58)(32)	
$B_{B_q}^{(2)}(\overline{m}_b)$	0.761(68)(33)	0.808(72)(35)	0.806(52)(27)	0.859(55)(29)
$B_{B_q}^{(3)}(\overline{m}_b)$	1.07(21)(5)	1.07(21)(5)	1.10(15)(4)	1.09(15)(4)
$B_{B_q}^{(4)}(\overline{m}_b)$	1.040(75)(45)		1.022(57)(34)	
$B_{B_q}^{(5)}(\overline{m}_b)$	0.964(93)(42)		0.943(68)(31)	
$B_{B_q}^{(2)}/B_{B_q}^{(1)}$	0.838(81)	0.885(73)	0.849(56)	0.902(59)
$B_{B_q}^{(3)}/B_{B_q}^{(1)}$	1.18(24)	1.17(24)	1.16(16)	1.15(16)
$B_{B_q}^{(4)}/B_{B_q}^{(1)}$	1.14(10)		1.073(68)	
$B_{B_q}^{(5)}/B_{B_q}^{(1)}$	1.06(11)		0.990(75)	

Bag-factor definitions

$$\langle \bar{B}^0 | \mathcal{O}_1 | B^0 \rangle = \tfrac{2}{3} f_B^2 M_B^2 B_B^{(1)}$$

$$\langle \bar{B}^0 | \mathcal{O}_2 | B^0 \rangle = -\tfrac{5}{12} \left(\frac{M_B}{m_b(\mu) + m_q(\mu)} \right)^2 f_B^2 M_B^2 B_B^{(2)}$$

$$\langle \bar{B}^0 | \mathcal{O}_3 | B^0 \rangle = \tfrac{1}{12} \left(\frac{M_B}{m_b(\mu) + m_q(\mu)} \right)^2 f_B^2 M_B^2 B_B^{(3)}$$

$$\langle \bar{B}^0 | \mathcal{O}_4 | B^0 \rangle = \left[\tfrac{1}{12} + \tfrac{1}{2} \left(\frac{M_B}{m_b(\mu) + m_q(\mu)} \right)^2 \right] f_B^2 M_B^2 B_B^{(4)}$$

$$\langle \bar{B}^0 | \mathcal{O}_5 | B^0 \rangle = \left[\tfrac{1}{4} + \tfrac{1}{6} \left(\frac{M_B}{m_b(\mu) + m_q(\mu)} \right)^2 \right] f_B^2 M_B^2 B_B^{(5)}$$

Two- and three-point correlator fits

M_{Bq} vs. t
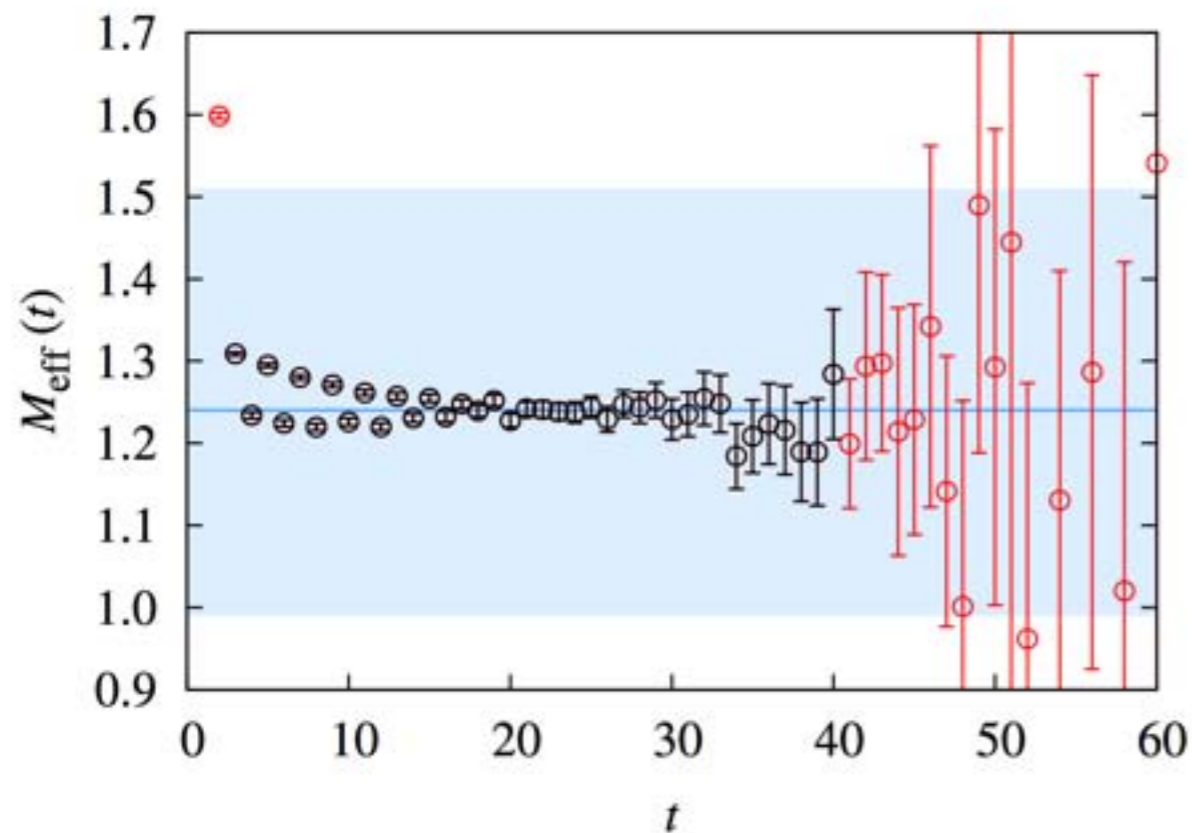
∘,∘: data, fit region
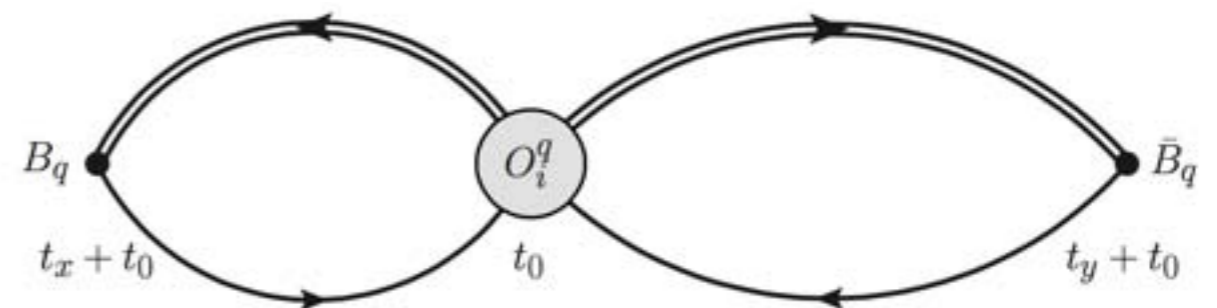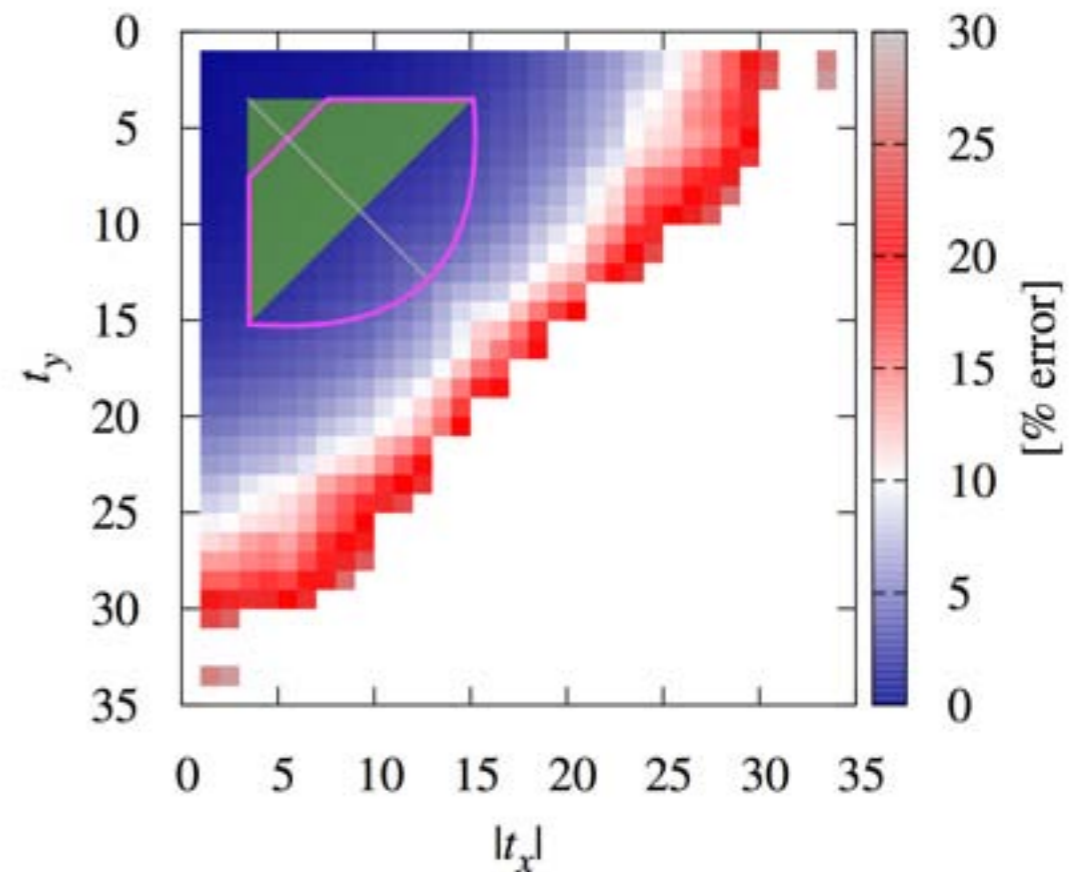▪,▪: prior, fit result

% error in $\langle O_2 \rangle$

- Constrained fits to correlation functions with wide priors that cover spread of data.

- Fit 3-point dependence on both B_q- & $\bar{B}_q$-meson locations t_x & t_y.

Operator matching & renormalization

Renormalize and match lattice operators to continuum $\overline{\text{MS}}$-NDR scheme using mostly nonperturbative renormalization (mNPR):

$$\mathcal{O}_i = Z_{V_{bb}^4} Z_{V_{dd}^4} \rho_{ij} O_j + \mathrm{O}(\alpha_s a, a^2)$$

- nonperturbative Z_{Vqq}s remove wave-function factors, tadpoles, and some vertex corrections.
- remaining factor ρ_{ij} is close to unity and computed at 1-loop in lattice perturbation theory.
- 2-loop perturbative corrections incorporated in chiral-continuum fit.

Operators $O_{1,2,3}$ & $O_{4,5}$ mix under renormalization.

Stability of $\langle O_4 \rangle$ under fit variations

- f_K instead of f_π

- vary operator renormalization

- vary data, χPT terms, prior widths

- vary discretization terms included

- "dumb" fits
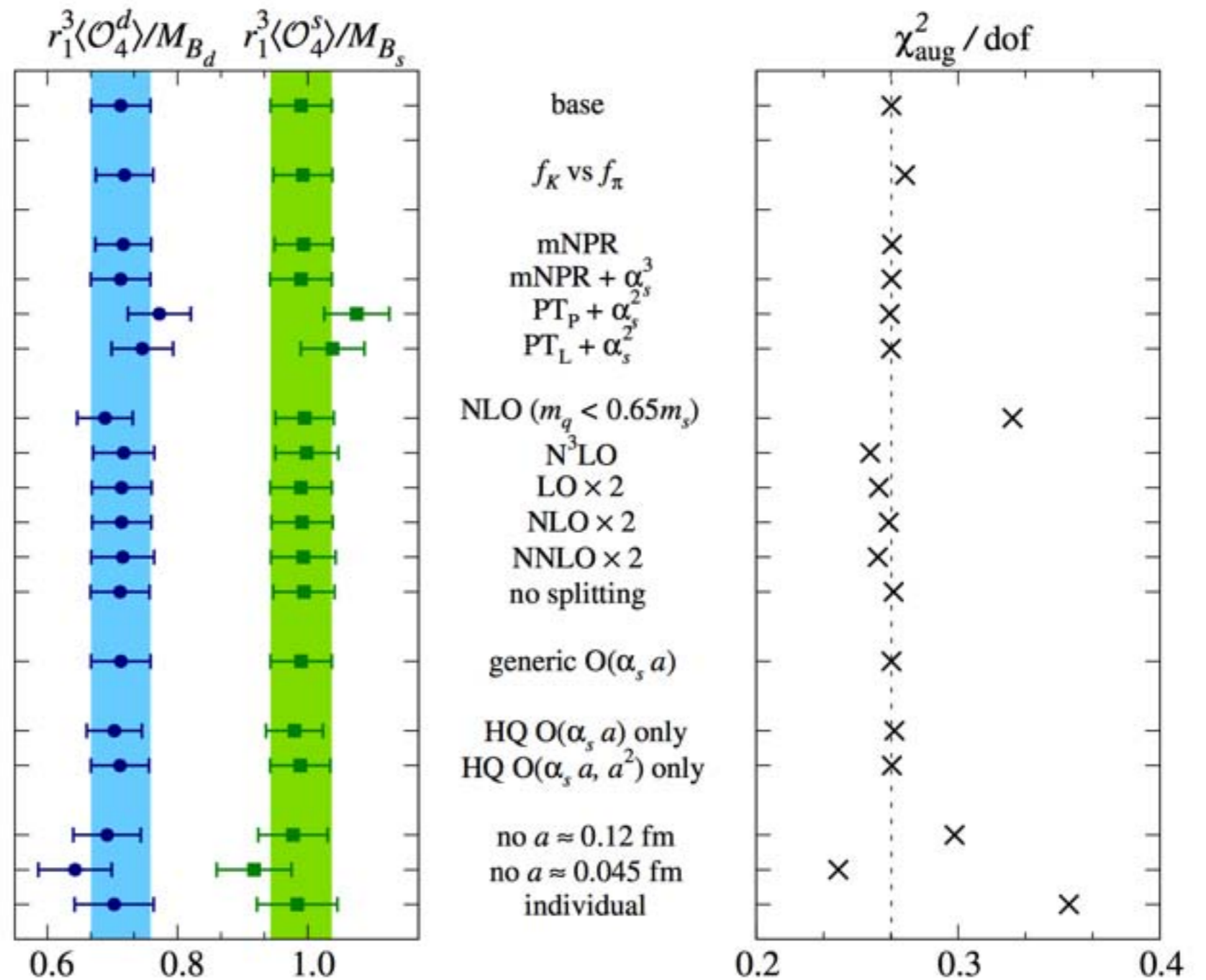
Approximate breakdown of fit error

TABLE IX. Breakdown of the chiral-continuum fit error. The labels and estimation procedure are described in the text. Entries are in percent.

	statistics	inputs	κ tuning	matching	chiral	LQ disc	HQ disc	fit total
$\langle \mathcal{O}_1^d \rangle$	4.2	0.4	2.1	3.2	2.3	0.6	4.6	7.7
$\langle \mathcal{O}_2^d \rangle$	4.6	0.3	1.1	3.7	2.6	0.6	4.6	8.0
$\langle \mathcal{O}_3^d \rangle$	8.7	0.2	2.1	12.6	4.8	1.2	9.9	19.0
$\langle \mathcal{O}_4^d \rangle$	3.7	0.4	1.7	2.2	1.9	0.5	3.9	6.4
$\langle \mathcal{O}_5^d \rangle$	4.7	0.5	2.5	4.7	2.7	0.8	4.9	9.1
$\langle \mathcal{O}_1^s \rangle$	2.9	0.4	1.5	2.1	1.6	0.4	3.2	5.4
$\langle \mathcal{O}_2^s \rangle$	3.1	0.3	0.8	2.5	1.6	0.4	3.1	5.5
$\langle \mathcal{O}_3^s \rangle$	5.9	0.3	1.4	8.6	3.0	0.7	6.9	13.0
$\langle \mathcal{O}_4^s \rangle$	2.7	0.4	1.2	1.6	1.3	0.3	2.9	4.8
$\langle \mathcal{O}_5^s \rangle$	3.4	0.4	1.8	3.4	1.9	0.5	3.6	6.7
ξ	0.8	0.4	0.3	0.5	0.4	0.1	0.7	1.4

Total error budget

TABLE XI. Total error budget for matrix elements converted to physical units of GeV^3 and for the dimensionless ratio ξ. The error from isospin breaking, which is estimated to be negligible at our current level of precision is not shown. Entries are in percent.

	Fit total	FV	r_1/a	r_1	EM	Total	Charm sea
$\langle \mathcal{O}_1^d \rangle / M_{B_d}$	7.7	0.2	2.5	2.1	0.2	8.3	2.0
$\langle \mathcal{O}_2^d \rangle / M_{B_d}$	8.0	0.3	2.8	2.1	0.2	8.8	2.0
$\langle \mathcal{O}_3^d \rangle / M_{B_d}$	19.0	< 0.1	2.5	2.1	0.2	19.3	2.0
$\langle \mathcal{O}_4^d \rangle / M_{B_d}$	6.4	< 0.1	2.1	2.1	0.2	7.1	2.0
$\langle \mathcal{O}_5^d \rangle / M_{B_d}$	9.1	< 0.1	2.2	2.1	0.2	9.6	2.0
$\langle \mathcal{O}_1^s \rangle / M_{B_s}$	5.4	0.1	1.9	2.1	0.2	6.1	2.0
$\langle \mathcal{O}_2^s \rangle / M_{B_s}$	5.5	0.1	2.1	2.1	0.2	6.2	2.0
$\langle \mathcal{O}_3^s \rangle / M_{B_s}$	13.0	< 0.1	1.9	2.1	0.2	13.3	2.0
$\langle \mathcal{O}_4^s \rangle / M_{B_s}$	4.8	< 0.1	1.7	2.1	0.2	5.5	2.0
$\langle \mathcal{O}_5^s \rangle / M_{B_s}$	6.7	< 0.1	1.8	2.1	0.2	7.2	2.0
ξ	1.4	< 0.1	0.6	0	0.04	1.5	0.5